Elastic Scattering of 1.6-Mev Gamma Rays from H, Li, C, and Al Nuclei*

Luis W. Alvarez, Frank S. Crawford, Jr., and M. Lynn Stevenson

Radiation Laboratory and Department of Physics, University of California, Berkeley, California

(Received July 28, 1958)

The elastic scattering of 1.6-Mev gamma rays from H, Li, C, and Al has been measured at an angle of 124°. The ratios of the measured differential cross sections to the classical Thomson differential cross sections are 0.94 ± 0.16 for H, 0.92 ± 0.10 for Li, 1.06 ± 0.10 for C, and 1.15 ± 0.10 for Al. These results agree with the field-theory prediction that in the low photon-energy limit the cross section must approach the classical Thomson cross section.

I. INTRODUCTION

PREVIOUS experimental studies of the elastic scattering of low-energy gamma rays have for the most part been confined to the heavier elements.[1] One of the reasons for this is that the small cross sections for the several important processes involved all are strongly Z dependent, while the relatively huge cross section for Compton scattering by electrons increases directly with Z. Two problems confronting an experimenter who attempts to observe the Thomson scattering from protons are the following: (a) the differential cross section at 124° is only 1.55×10^{-32} cm² sterad⁻¹, so that one needs strong sources and efficient detectors to give counting rates above natural backgrounds; and (b) scattering from electrons is several million times more probable than it is from protons, so that extreme precautions must be taken to reduce the effects of electron-scattered quanta.

These experiments[2] have been made possible by two developments of the past decade. The availability of multicurie sources of artificially radioactive substances from chain-reacting piles has overcome the first difficulty, and the development of the large NaI-crystal counter has provided a solution to the second. The large NaI counter is essentially a total-energy-sensitive counter, which gives an output pulse proportional to the energy of the incident photon. This is in marked contrast to the older gas counters, which had no such energy-sensing properties. One makes use of the well-known fact that Compton-scattered photons at 90° all have an energy of approximately m_0c^2 if their initial energy was considerably higher than m_0c^2. The elastically scattered photons then give larger pulses than the Compton-scattered photons, and so should be recognizable by a properly biased electronic circuit. This description of the experimental technique is, of course, oversimplified; the details are described in the next section.

One might think that the calculation of the Thomson cross section for light nuclei is so straightforward that no new information could come from its measurement. One of our colleagues, on the basis of a theoretical model (which he later showed was in error), encouraged us to look in the range of radioactive gamma-ray energies for what he believed might be a substantial departure from the simple Thomson cross section. In any case, from the purely experimental point of view, it did seem worth while to search for an increased cross section due to scattering from the light, virtual mesons surrounding the nucleon core.

Actually, there exists a theorem from field theory that requires the scattering cross section to approach the classical Thomson cross section as the photon energy goes to zero.[3] The experimental results can be considered to substantiate the principles of Lorentz, gauge, and charge-conjugation invariance in which this theorem from renormalizable field theory is predicated.

At much higher photon energy, deviations from the Thomson cross section are expected. If one neglects the anomalous magnetic moment of the proton, the cross section is given by the Klein-Nishina formula. Powell has calculated the scattering taking into account the anomalous magnetic moment of the proton.[4] Measurements in the high-energy region just below photomeson threshold have been made by Oxley and Telegdi,[5] and by Janes et al.;[6] these agree with the Powell theory for 90° scattering but seem to fall below the predicted value for angles greater than 90°.

Fuller and Hayward have investigated elastic scattering on various elements from Na to U for gamma-ray energies between 4 and 40 Mev.[7] They observed two

* This research was performed under the auspices of U. S. Atomic Energy Commission.

[1] E. Pollard and D. E. Alburger, Phys. Rev. **74**, 926 (1948); A. Storruste, Proc. Phys. Soc. (London) **A63**, 1197 (1950); Robert R. Wilson, Phys. Rev. **90**, 720 (1953); Thomas D. Strickler, Phys. Rev. **92**, 923 (1953); W. G. Davey, Proc. Phys. Soc. (London) **A66**, 1059 (1953); J. L. Burkhardt, Phys. Rev. **100**, 192 (1955); S. Messelt and A. Storruste, Proc. Phys. Soc. (London) **A69**, 381 (1956); and Alfred K. Mann, Phys. Rev. **101**, 4 (1956).

[2] A preliminary report was given at the American Physical Society Meeting at Berkeley in 1954, and is summarized by the authors in Phys. Rev. **98**, 280(A) (1955).

[3] Walter Thirring, Phil. Mag. **41**, 1193 (1950); N. Kroll and M. Ruderman, Phys. Rev. **93**, 233 (1954); Francis E. Low, Phys. Rev. **96**, 1428 (1954); M. Gell-Mann and M. L. Goldberger, Phys. Rev. **96**, 1433 (1954); R. H. Capps and W. G. Halliday, Phys. Rev. **99**, 931 (1955); Abraham Klein, Phys. Rev. **99**, 998 (1955); and Karzas, Watson, and Zachariasen, Phys. Rev. **110**, 253 (1958).

[4] John L. Powell, Phys. Rev. **75**, 32 (1949). See also R. Gomez and D. Walecka, Phys. Rev. **104**, 1479 (1956), and Phys. Rev. **106**, 1371 (1957).

[5] C. L. Oxley and V. L. Telegdi, Phys. Rev. **100**, 435 (1955).

[6] Janes, Gomez, Pugh, and Frisch, Phys. Rev. **100**, 1245 (1955).

[7] E. G. Fuller and E. Hayward, Phys. Rev. **101**, 692 (1956).

H - LEAD SHIELDING
I - MOVABLE COLLIMATING SHIELD

A - RADIOACTIVE SOURCE, S_0
B - Li TARGET
C - LiH TARGET
D - 4" DIAM X 4" NaI
    CRYSTAL

E - STYROFOAM TARGET
    SUPPORTS
F - REMOTE CONTROLLED CART
    FOR CYCLING THE TARGETS
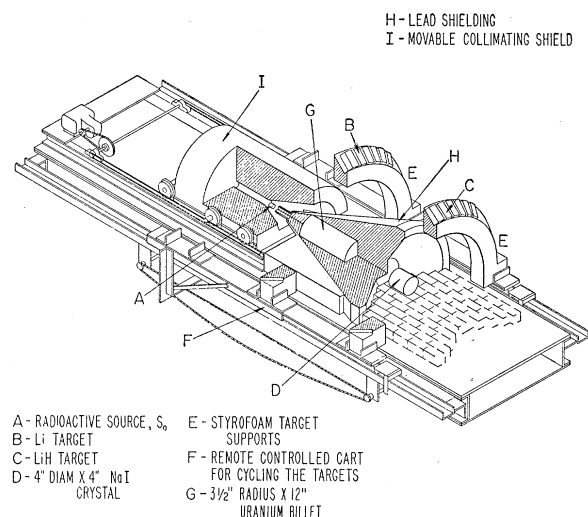G - 3½" RADIUS X 12"
    URANIUM BILLET

FIG. 1. Scattering geometry. The LiH and Li targets "C" and "B," respectively, are shown on their Styrofoam supports, E. The LiH target is shown in the scattering position. Not shown in this figure is the blank Styrofoam target, although the flanges that support the blank are shown. All three targets are mounted on an automatically controlled movable cart, F. When one target is in the scattering position, the other two targets are in a position such that neither the source, A, nor the detector, D, can "see" the other targets. The movable shield I remains fixed during a given run. A uranium cylinder, G, 7 inches in diameter and 12 inches long, prevents the source from directly irradiating the detector. The conical lead shield, H, shields the detector from air-scattered gamma rays.

maxima in the energy dependence that they feel indicate scattering by separate nuclear levels and by the "giant resonance" process.

II. EXPERIMENTAL DETAILS

Geometry

Figure 1 shows the experimental arrangement that was used in the course of this work. The scattering geometry had a horizontal axis of symmetry. The source of the gamma rays was placed at Position A. The source, when not in use, was shielded by placing the movable shield I in contact with the fixed conical shield H. When the source was in use, the shield I was moved back to the position shown in Fig. 1. A conical sheath of gamma rays radiated from the opening formed by the shields I and H, so as to completely bathe the ring-shaped target with photons. The shields I and H were so placed that the targets would be irradiated only when in the "in" position of target C and not when in the "out" position shown by target B. In addition to preventing gamma rays from striking the targets when in the out position, the conical collimation furnished by shields I and H restricted the zone in which air scattering could take place and hence reduced this form of background.

The gamma rays that scattered from the target C into the detector D, were deflected by $124\pm3°$. The detector was a NaI crystal 4 in. in diameter and 4 in.

long, viewed by a 5-in.-diameter photomultiplier tube. The photomultiplier (not shown in Fig. 1) and the crystal were located on the axis. A lead filter (not shown) in the form of a coaxial cylindrical lead sheet of variable thickness was placed between the detector and the scatterer. If insufficient filter were used, the very strong flux of 0.3-Mev photons from the Compton scattering from electrons would, through accidental coincidences, shift and broaden the pulse-height spectrum of the elastically scattered gammas and make pulse-height analysis impossible. The lead filter produced a differential absorption effect; the Compton-scattered photons of 0.3 Mev were attenuated much more effectively than the nuclear-scattered gammas with the full energy of 1.6 Mev. The optimum thickness of lead varied between $\frac{1}{2}$ in. and $\frac{3}{4}$ in., depending upon the source intensity and the scattering material, and provided a relative filtering action of 4×10^6($\frac{1}{2}$ in.) to 7×10^9 ($\frac{3}{4}$ in.).

The massive absorber between the source and the detector consisted of a uranium cylinder 7 in. in diameter and 12 in. long. In order to shield the counter from the gamma rays and neutrons emitted from the uranium, 8 inches of lead was placed between the uranium and the detector. The additional lead shown near the head of the arrow H in Fig. 1 eliminated plural Compton scattering from electrons in air atoms, which could otherwise carry a gamma ray around the uranium from the source to the detector without substantial energy loss. Additional lead was placed underneath the table that supported the semicylindrical geometry. Because the apparatus was located on the roof of the laboratory, this additional shielding was necessary both as a health measure, and to eliminate background in low-level counting experiments in the rooms below.

The value of the scattering cross section is calculated in terms of several measured ratios, plus two macroscopic measurements—one of length and the other of mass. No measurement of source strength, nor of absolute counting rate is required. The strong source was put into solution, and aliquot ratios of 10^{-6}, 10^{-7}, and 10^{-8} were prepared. This was easily done by taking a 10^{-2} sample of the original source that was in solution and dissolving it in the same volume of water. This operation was repeated twice to obtain the 10^{-6} sample. Similar procedures were used to obtain the other aliquots of 10^{-7} and 10^{-8}. The aliquots were placed in small vials with walls of negligible thickness. One of the vials, the choice of which depended upon the thickness of the filter, was then placed at the same average position as the target. The counting rates produced by the scattered photons plus the direct photons from the aliquot were measured; the aliquot was then removed and the counting rate was measured for scattered photons only. By subtraction, one obtains the counts produced by the aliquot alone. The reason for obtaining the aliquot counts by subtraction is to

reproduce the same "pile-up" distortion (if any) of the pulse-height spectrum for the aliquot measurement as for the scattered-gamma-ray measurement.[8] The scattered-gamma-ray counts are obtained by subtracting the counts obtained with a blank target from the counts obtained during an equal amount of running time with the target "in." The ratio of scattered-gamma-ray counts to aliquot counts thus obtained is called R. The distance, L, from the source (A) to the target (C) was then measured with a meter stick. Finally, the mass M of the scatterer yields the number of atoms responsible for the scattering. The differential scattering cross section is then

$$d\sigma/d\Omega = rL^2RA/MN_{Av}, \qquad (1)$$

where A is the atomic weight, and N_{Av} is Avogadro's number. Typically, when the aliquot ratio r was 10^{-7}, the counting-rate ratio R was of the order of 10^{-2}.

In practice there are small corrections to be made to Eq. (1) to take into account (a) the photon attenuation upon entering and leaving the scatterer, (b) the attenuation in the primary-source holder, (c) the attenuation of the "aliquot" photons in the vials, (d) the change in average scattering angle for targets of different thickness, (e) the fact that the calibration counts were not taken at exactly the same time as the scattered counts, and (f) bremsstrahlung effects present in the scattered photon spectrum but not in the "aliquot" spectrum. Actually, in determining cross sections, we consider only that part of the pulse-height
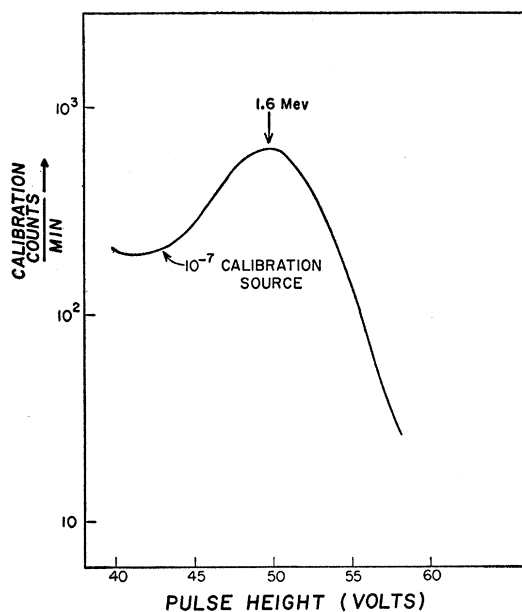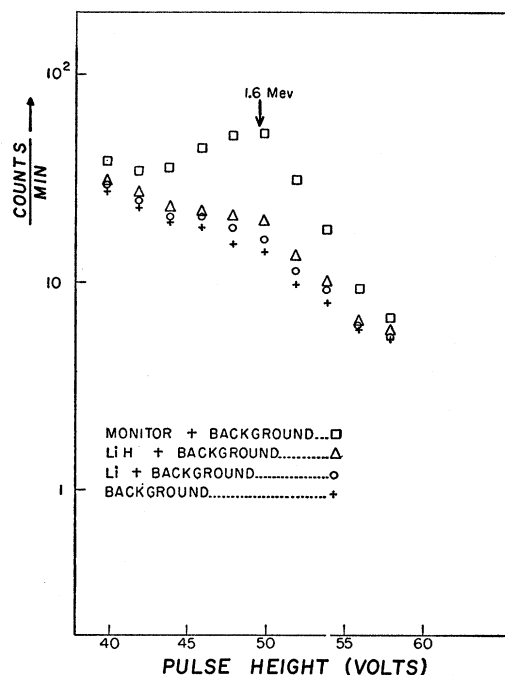

FIG. 3. Pulse-height distributions prior to background subtraction. This figure shows the relative contributions to the total counting rate by Li, H, and background. One can see that the contribution of the H and Li scatterers to the total counting rate is small compared with the background.

spectrum where the bremsstrahlung effects are visibly negligible. We list it as a correction only to emphasize that we are aware of the effects. (For an excellent discussion of these latter effects, see Messelt and Storruste.[1])

The thickness of the scatterer was limited by the magnitude of the first correction factor. We restricted the target thicknesses sufficiently to keep all calculated absorption corrections below 20%.

Source

The choice of the primary source of gamma rays was governed by several factors. First, it was desirable, from the standpoint of reducing possible distortion of the pulse-height spectrum due to accidental coincidences with Compton-scattering photons, to use as high a gamma-ray energy as possible. The relative filtering action of the lead filter improves drastically with increased photon enenergy. Second, the source had to have a half-life of the order of a week or two to allow sufficient time to perform the measurements and to check those measurements. Third, the source had to be available in multicurie quantities at reasonable prices.

The source that was finally used in this work consisted of approximately 100 curies of Ba^{140}-La^{140}. This source emits among other things a 0.5-Mev gamma ray of 20% abundance, a 1.6-Mev gamma ray of 60% abundance, and a 2.5-Mev gamma ray of 3% abun-

FIG. 2. Pulse-height distribution of the Ba^{140}-La^{140} source near the 1.6-Mev gamma-ray peak. The distribution was obtained by placing a 10^{-7} aliquot of the main source at the target position.

[8] There was actually no distortion of the spectrum caused by pileup, but the precaution was taken nevertheless.
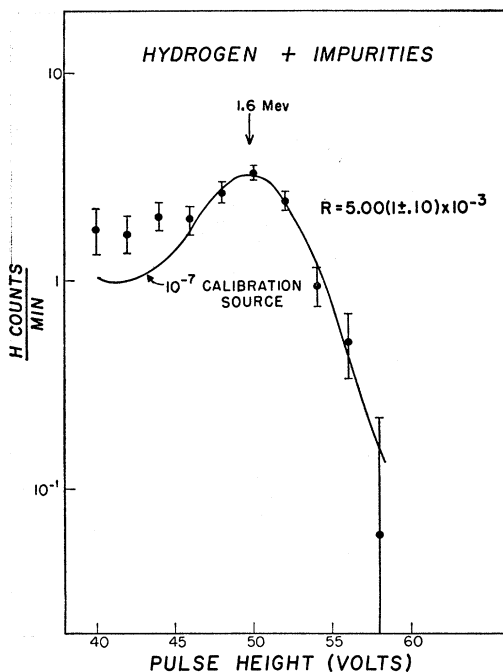
FIG. 4. Uncorrected hydrogen pulse-height distribution. This figure shows the pulse-height distribution after the Li-plus-background counts are subtracted from the LiH-plus-background counts. Sixty percent of the resulting counts come from "impurities" that were in the LiH tagret but not in the Li target. The remaining 40% of the counts are from photon-hydrogen scatters. Also shown in this figure is the 10^{-7} calibration source pulse-height distribution, which has been multiplied by the factor $R=5.00(1\pm0.10)\times10^{3^3}$ so as to coincide with the scattered distribution near the peak.
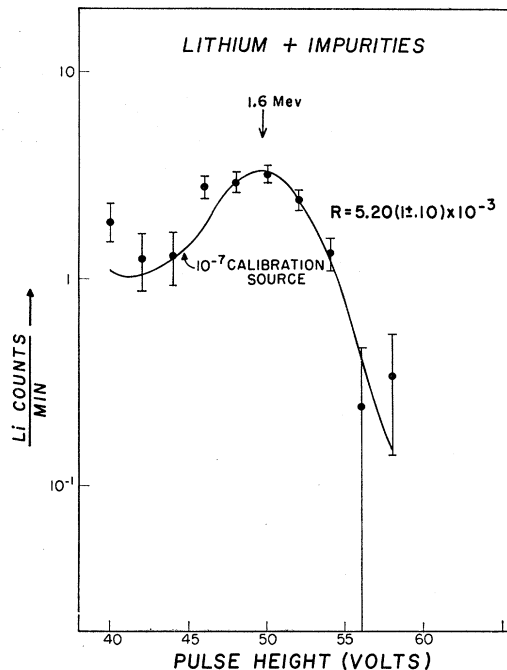
FIG. 5. Uncorrected lithium pulse-height distribution. The pulse-height distribution after subtraction of background counts from the Li-plus-background counts is shown. Twelve percent of the resulting counts come from "impurities" in the Li target that were not in the blank target. The remaining 88% of the counts are from photon-Li scatters. Here the 10^{-7} calibration distribution has been shifted by a factor $R=5.20(1\pm0.10)\times10^{-3}$ so as to agree with the scattered distribution near the peak.

dance. The half-life is 12.8 days. The cross-section measurements were made with the 1.6-Mev gamma ray. Figure 2 shows the sodium iodide pulse-height distribution in the vicinity of the 1.6-Mev gamma-ray peak. This distribution was obtained by placing the 10^{-7} aliquot of the main source at the target position C.

Electronics

The scattered photons were detected when they converted in the NaI crystal via Compton scattering, pair production, or photoelectric effect. The resulting pulses from the 5-in.-diameter photomultiplier were amplified and then counted with a 10-channel pulse-height analyzer. The 10 channels could be set to sample any desired portion of the pulse-height distribution. The horizontal separation between any two adjacent points in Figs. 3 to 7 corresponds to a channel width of 2 volts. To minimize thermal drifts, as much of the electronic apparatus as possible was placed in an air-conditioned room. However, the photo tube necessarily had to be placed outside where there were wide variations in temperature. Consequently, steps had to be taken to compensate for the appreciable drifts which occurred over approximately 12-hr periods. We overcame these long-time drifts by using a feedback amplifier

and servomechanism in the following way. We periodically, and automatically, exposed the NaI crystal directly to an aliquot of the main source which we refer to as the monitor source. At the same time, we switched the phototube output from the 10-channel analyzer to a single-channel pulse-height analyzer. The single-channel analyzer was set to sample the counting rate on the steepest part of the 0.5-Mev photon pulse-height distribution. This counting rate was so large that the single-channel pulse-height analyzer acted as a source of dc current. When the amplification in the crystal plus phototube changed by a slight amount, a large change in the dc current was produced. The difference in dc current was fed into a difference amplifier as a source of feedback and thence to a servomotor which controlled the gain on the linear amplifier. The feedback system then maintained the counting rate on the steep slope of the distribution constant by varying the linear-amplifier gain. This in turn kept the pulse-height distribution fixed.

The necessity for such precautions can be appreciated when one observes that in the case of hydrogen, we were detecting a difference in counting rate between LiH and Li of about 40% of the Li counting rate, which in turn was only about 20% above background. In order to obtain sufficient statistical accuracy, the dura-

tion of the counting times of single runs were in some instances as long as 24 hr.

The counts induced by 1.6-Mev gamma ray from the monitor source were accumulated in a separate bank of registers and provided us with a check against drifts.

In order to further minimize systematic errors due to drifts, an elaborate method of target cycling was used. A typical target cycle is represented symbolically as follows[9]:

$$L(\tfrac{1}{2}),\ M(\tfrac{1}{3}),\ B(2),\ M(\tfrac{1}{3}),\ L(\tfrac{1}{2}),$$

$$M(\tfrac{1}{3}),\ H(\tfrac{1}{2}),\ M(\tfrac{1}{3}),\ H(\tfrac{1}{2}),\ M^*(\tfrac{1}{3}),$$

repeat. L, M, B, and H represent the Li target, monitor source, blank target,[10] and the LiH target, respectively. The quantities in parentheses indicate the time in minutes that the particular target (or source) was in place. The Li, LiH, blank, and monitor counts were accumulated in four separate banks of ten scaling registers each. Each register bank was provided with a clock which recorded its integrated "on" time. About three times during each run the aliquot source was placed in position C, and a calibration run of a few
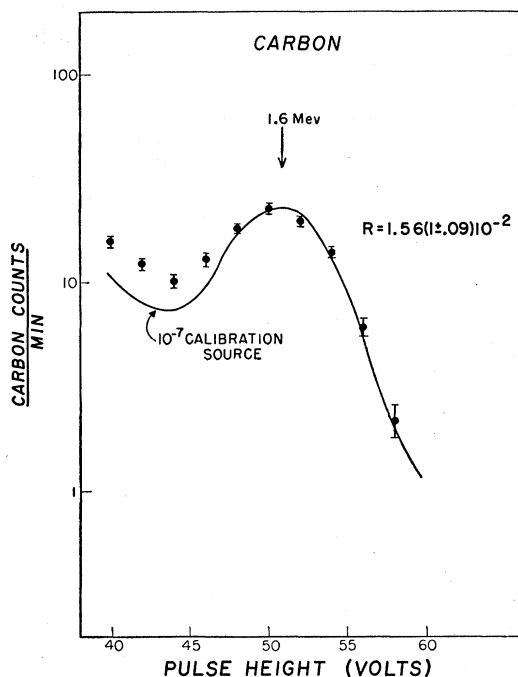

FIG. 6. Carbon pulse-height distribution. The C pulse-height distribution after background subtraction is shown. Here the 10^{-7} calibration distribution has been shifted by a factor $R=1.56(1\pm0.09)\times10^{-2}$ so as to agree with the scattered distribution near the peak.

---

[9] The last monitor run (M^*) of each cycle was used by the servomechanism to compensate for any drifts that occurred during the cycle.

[10] The blank is not shown in Fig. 1 in order to avoid complication of the drawing. However, the flanges that supported the Styrofoam blank target are shown on the cart that contains the other two targets.
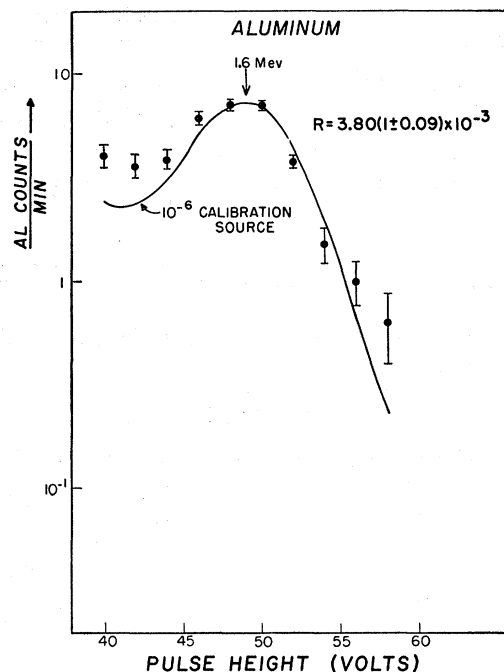

FIG. 7. Aluminum pulse-height distribution. This figure shows the Al pulse-height distributions after background subtraction. Shown also is the 10^{-6} calibration distribution that has been shifted by the factor $R=3.80(1\pm0.09)\times10^{-3}$.

minutes duration was made. The pulse-height spectrum obtained from the aliquot source was then compared with that obtained from the accumulated monitor counts to insure that no drifts had occurred.

III. MEASUREMENTS

Figure 3 shows for a typical run the pulse-height distributions obtained from LiH, Li, and the monitor source, prior to background subtraction. The background is also shown. The curves give the actual counting rates in this particular run in counts/min.

That one is detecting elastically scattered gamma rays is evident from the similarity of the "scattered gamma ray" pulse-height distribution to those obtained from the aliquot source. The target-out curve also shows a slight peak corresponding to elastic scattering of 1.6-Mev photons from air nuclei. The most striking dissimilarity in the curves in the presence of an excess of small pulse heights in the scattered photon distribution not present in the aliquot distributions. We believe this difference to be caused indirectly by electrons ejected from the atoms of the target with almost the same energy as the primary photon. These high-energy electrons undergo several scatters and subsequently radiate bremsstrahlung photons into the detector. The effect of these photons is to produce a high-energy tail which partially fills in the valley present in the unscattered aliquot distribution. For this reason, only channels 5 through 8, which are sub-

TABLE I. Summary of cross sections and corrections.

Element	Lead-filter thickness (inch)	r of cali-bration source	$R \times 10^3$ uncorrected	$d\sigma/d\Omega$ uncorrected $(10^{-32}$ cm$^2)$	Correction factors						$d\sigma/d\Omega$ corrected $(10^{-32}$ cm$^2)$	$\left(\dfrac{d\sigma/d\Omega_Z}{d\sigma/d\Omega(\text{Thomson})}\right)$
					Attenuation			Finite target thickness	Relative decay of sources	Target impu-rities		
					Target	Source holder	Aliquot vial					
H	1/2	10^{-7}	5.00(1±0.10)	2.00(1±0.10)	1.18	1.03	0.96	0.97	1.04	0.63	1.45(1±0.17)	0.94(1±0.17)
Li $(A = 6.94)$	1/2	10^{-7}	5.20(1±0.10)	2.28(1±0.10)	1.18	1.03	0.96	0.97	1.04	0.89	2.39(1±0.11)	0.92(1±0.11)
C	1/2	10^{-7}	15.6(1±0.09)	13.4(1±0.09)	1.12	1.03	0.96	1.00	1.00	1.00	14.9(1±0.10)	1.06(1±0.10)
Al	3/4	10^{-6}	3.80(1±0.09)	65.4(1±0.09)	1.14	1.03	0.96	1.00	0.94[a]	1.00	69.2(1±0.10)	1.15(1±0.10)

[a] This correction includes a 5% correction in the relative source strengths of the 10^{-6} and the 10^{-7} aliquots, and a small geometrical correction that takes into account the fact that the calibration source was not placed exactly at the average position of the target.

stantially above the tail, were used in the cross section determinations.†

Hydrogen Cross Section

The hydrogen cross section was obtained by a LiH-Li subtraction. The lead filter used was $\frac{1}{2}$ in. thick. The LiH and Li targets consisted of 25 individual 2- by 2-by 4-in. blocks on a Styrofoam support in the semi-circular arrangement shown in Fig. 1. The LiH target contained a total of 569 moles of H, 513 moles of Li, 31.8 moles of C, and 7.43 moles of O. The C and O impurities were contained in the plastic binder that held the LiH together and in the Saran wrap and masking tape used to keep moisture from the LiH.

The Li target contained 9.48 moles of H, 514 moles of Li, 4.74 moles of C, and 2.2±1.4 moles of O. The C and H impurities are from the Saran wrap and masking tape. The oxygen was due to a small layer of oxidized lithium on the surface of the targets which was caused by moisture that penetrated the protective wrapping.

The total counts obtained from the Li target are subtracted from those obtained from the LiH target to give the counts produced by the hydrogen plus the impurities. Figure 4 shows the pulse-height distribution of the hydrogen plus impurities. The contribution from the impurities is calculated using the theoretical Thomson cross sections for C and O. This correction is 60% of the hydrogen contribution.[11] Also shown in Fig. 4, as a solid line, is the pulse-height distribution from the calibration source $(r = 10^{-7})$. The absolute value must be shifted vertically by a factor $R = 5.00 \times (1 \pm 0.10) \times 10^{-3}$ so as to fit the observed distribution in the vicinity of the peak. The measured distance L is 1.17 meters. The number of nuclei within the target is 3.36×10^{26}, so that Eq. (1) becomes

$$d\sigma/d\Omega = 405R \times 10^{-32} \text{ cm}^2 \text{ sterad}^{-1}.$$

The resulting uncorrected cross section is 2.03(1±0.10) $\times 10^{-32}$ cm^2 sterad^{-1}. Table I summarizes the correc-

† *Note added in proof.*—Similarly, the 2.5-Mev γ ray can produce Compton electrons which radiate 1.6-Mev photons into the detector. We estimate that at most 1% of the counts in Channels 5 through 8 are caused by the 2.5-Mev γ ray. No correction was made for this effect.

[11] The carbon cross section was measured later in the experiment and agrees with the theoretical Thomson cross section (see later section).

tions that were made to obtain the corrected cross section for hydrogen,

$$\frac{d\sigma}{d\Omega_H}(124°) = 1.45(1\pm0.17) \times 10^{-32} \text{ cm}^2 \text{ sterad}^{-1}.$$

which is equivalent to

$$\frac{d\sigma}{d\Omega}(124°) \Big/ \left(\frac{d\sigma}{d\Omega}\right)_{\text{Thomson, H}} = 0.94(1\pm0.17).$$

Lithium Cross Section

After the background counts are subtracted from the Li target counts, we obtain the pulse-height distribution shown in Fig. 5. The solid curve represents the 10^{-7} aliquot distribution which this time has been shifted by a factor $R = 5.20(1\pm0.10) \times 10^{-3}$ to fit the observed counts near the peak. After making the corrections summarized in Table I, we obtain for the normal isotopic mixture of Li$(A = 6.94)$ the cross section

$$\frac{d\sigma}{d\Omega_{Li}}(124°) = 2.39(1\pm0.11) \times 10^{-32} \text{ cm}^2 \text{ sterad}^{-1},$$

or

$$\frac{d\sigma}{d\Omega_{Li}}(124°) \Big/ \left(\frac{d\sigma}{d\Omega}\right)_{\text{Thomson, Li}^{6.94}} = 0.91(1\pm0.11).$$

Carbon Cross Section

Figure 6 shows the counts from a $\frac{1}{2}$-inch-thick carbon target after background has been subtracted. The calibration source was the 10^{-7} aliquot. In this particular run, $R = 1.56(1\pm0.09) \times 10^{-2}$. When we average this result with other similar results and make the corrections of Table I, we obtain

$$\frac{d\sigma}{d\Omega_C}(124°) = 14.9(1\pm0.10) \times 10^{-32} \text{ cm}^2 \text{ sterad}^{-1},$$

or

$$\frac{d\sigma}{d\Omega_C}(124°) \Big/ \left(\frac{d\sigma}{d\Omega}\right)_{\text{Thomson, C}} = 1.06(1\pm0.10).$$

Aluminum Cross Section

The Al target was $\frac{3}{8}$ in. thick, the lead filter $\frac{3}{4}$ in. thick. Figure 7 shows the distribution of scattered photons after background subtraction. The calibration source was shifted by $R = 3.80(1 \pm 0.09) \times 10^{-3}$. After making the corrections shown in Table I, we obtain

$$\frac{d\sigma}{d\Omega_{Al}}(124°) = 69.2(1 \pm 0.10) \times 10^{-32} \text{ cm}^2 \text{ sterad}^{-1},$$

or

$$\frac{d\sigma}{d\Omega_{Al}}(124°) \Big/ \left(\frac{d\sigma}{d\Omega}\right)_{Thomson, Al} = 1.15(1 \pm 0.10).$$

IV. DISCUSSION OF RESULTS

The Z dependence of the cross sections at 1.6 Mev is summarized in Fig. 8. The measured differential cross sections are plotted in units of 10^{-32} cm²/sterad as solid circles; the ratios of the measured cross section to the classical Thomson cross section are plotted as open circles. Our result—that the measured hydrogen cross section is equal to the Thomson cross section (within the experimental error)—verifies a prediction of the low-energy theorem of renormalizable-field theory.[3] This theorem, which is based upon Lorentz,

Fig. 8. Z dependence of the elastic scattering cross section at 124° for 1.6-Mev gamma rays. The solid circles give the differential cross section as a function of Z. The open circles are ratios of the measured cross sections to the classical Thomson cross sections. These ratios are statisically consistent with unity, which shows that the scattering under these conditions can be adequately explained by the classical Thomson process.

gauge, and charge-conjugation invariance, states that as the photon energy approaches zero, the scattering cross section must approach the classical Thomson cross section. Low photon energy is that which is small compared with the pion rest energy. In this limit, it appears that the classical description of the scattering process is adequate. When one tries to extend this theorem to more complex nuclei, the effects of Rayleigh scattering from the bound electrons, and of virtual pair production in the field of the nucleus (Delbrück scattering), which are unimportant for hydrogen, become complicating factors. Brown and Woodward[12] point out that the calculation of the Rayleight scattering from a complex atomic system is a formidable task for the general case where large momentum transfers are involved. The calculation of Delbrück scattering likewise has been made only for small momentum transfers.[13,14] Our experimental results for Li, C, and Al indicate that for large momentum transfers (124° deflection) the scattering is still predominantly Thomson scattering. However, as Z increases, the electrons become more tightly bound, and the Rayleigh scattering, which increases roughly as the eighth to tenth power of Z for large momentum transfer,[15] becomes more important. At the same time the Delbrück scattering is increasing as Z^4 so that all three amplitudes, Thomson, Rayleigh, and Delbrück, interfere in some quantitatively unknown fashion. Qualitatively, theory predicts that the scattering amplitudes for Thomson and Rayleigh processes interfere constructively with each other and both interfere destructively with the Delbrück scattering amplitude.[13,14] As long as the calculations of Rayleigh scattering and Delbrück scattering remain inadequate, there seems to be little hope of unscrambling these three processes with any quantitative accuracy.
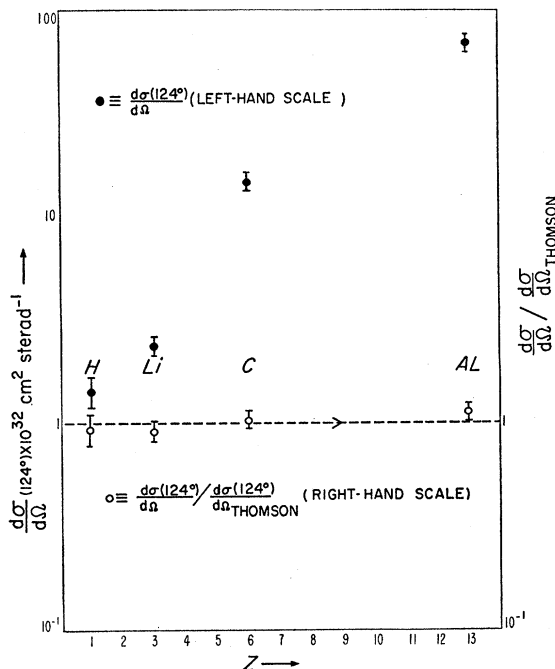
[12] G. Brown and J. Woodward, Proc. Phys. Soc. (London) A65, 977 (1952).
[13] F. Rohrlich and R. L. Gluckstern, Phys. Rev. 86, 1 (1952).
[14] H. A. Bethe and F. Rohrlich, Phys. Rev. 86, 10 (1952).
[15] Hans A. Bethe, private communication to R. Wilson, Phys. Rev. 90, 720 (1953).